Seedling root system adaptation to water availability during maiden domestication and global expansion

# Seedling root system adaptation to water availability during maize domestication and global expansion

Peng Yu[1,2,#,*], Chunhui Li[3,#], Meng Li[4,#], Xiaoming He[1,2,#], Danning Wang[1,2], Hongjie Li[1,2], Caroline Marcon[1], Yu Li[3], Sergio Perez-Limón[4], Xinping Chen[5], Manuel Delgado-Baquerizo[6,7], Robert Koller[8], Ralf Metzner[8], Dagmar van Dusschoten[8], Daniel Pflugfelder[8], Ljudmilla Borisjuk[9], Iaroslav Plutenko[9], Audrey Mahon[10], Marcio F.R. Resende Jr.[10], Silvio Salvi[11], Asegidew Akale[12], Mohanned Abdalla[12], Mutez Ali Ahmed[12], Felix Maximilian Bauer[13], Andrea Schnepf[13], Guillaume Lobet[13,14], Adrien Heymans[14], Kiran Suresh[15], Lukas Schreiber[15], Chloee M. McLaughlin[16], Chunjian Li[17], Manfred Mayer[18], Chris-Carolin Schön[18], Vivian Bernau[19], Nicolaus von Wirén[20], Ruairidh J. H. Sawers[4,*], Tianyu Wang[3,*], Frank Hochholdinger[1,*]

[1] Crop Functional Genomics, Institute of Crop Science and Resource Conservation (INRES), University of Bonn, 53113 Bonn, Germany
[2] Emmy Noether Group Root Functional Biology, Institute of Crop Science and Resource Conservation (INRES), University of Bonn, 53113 Bonn, Germany
[3] State Key Laboratory of Crop Gene Resources and Breeding, Institute of Crop Sciences, Chinese Academy of Agricultural Sciences, 100081 Beijing, China
[4] Department of Plant Science, Pennsylvania State University, State College, Pennsylvania, USA
[5] College of Resources and Environment, and Academy of Agricultural Sciences, Southwest University (SWU), 400715 Chongqing, P. R. China
[6] Laboratorio de Biodiversidad y Funcionamiento Ecosistémico. Instituto de Recursos Naturales y Agrobiología de Sevilla (IRNAS), CSIC, Av. Reina Mercedes 10, E-41012, Sevilla, Spain
[7] Unidad Asociada CSIC-UPO (BioFun). Universidad Pablo de Olavide, 41013 Sevilla, Spain
[8] Institute of Bio- and Geosciences, Plant Sciences (IBG-2), Forschungszentrum Juelich GmbH, 52425 23 Juelich, Germany
[9] Leibniz Institute of Plant Genetics and Crop Plant Research (IPK), Stadt Seeland, Germany
[10] Horticultural Sciences Department, University of Florida, Gainesville, FL, USA
[11] Department of Agricultural and Food Sciences, University of Bologna, 40127 Bologna, Italy
[12] Chair of Root-Soil Interactions, TUM School of Life Sciences, Technical University of Munich, Freising, Germany
[13] Institute of Bio-and Geosciences, Agrosphere (IBG-3), Forschungszentrum Jülich GmbH, 52425 Jülich, Germany
[14] Earth and Life Institute, Université catholique de Louvain, Belgium
[15] Institute of Cellular and Molecular Botany (IZMB), Department of Ecophysiology, University of Bonn, Bonn, Germany
[16] Intercollege Graduate Degree Program in Plant Biology, The Pennsylvania State University, State College, Pennsylvania, USA
[17] Key Laboratory of Plant-Soil Interactions, College of Resources and Environmental Sciences, National Academy of Agriculture Green Development, Ministry of Education, China Agricultural University, Beijing, P. R. China
[18] Plant Breeding, TUM School of Life Sciences, Technical University of Munich, Freising, Germany
[19] North Central Regional Plant Introduction Station, USDA-Agriculture Research Service and Iowa State University, Ames, Iowa, USA
[20] Department of Physiology and Cell Biology, Leibniz Institute of Plant Genetics and Crop Plant Research (IPK), 06466 Gatersleben, Germany

[#] These authors equally contributed to this work.

[*] To whom correspondence should be addressed:

yupeng@uni-bonn.de
rjs6686@psu.edu
wangtianyu@caas.cn
hochholdinger@uni-bonn.de

## One sentence summary

We demonstrated that fewer seminal roots in maize are beneficial under drought and identified genes controlling their environmental variation.

## Abstract

The maize root system has been reshaped by indirect selection during global adaptation to new agricultural environments. In this study, we characterized the root systems of >9,000 global maize accessions and its wild-relatives, defining the geographical signature and genomic basis of variation in seminal root number. We demonstrate that seminal root number has increased during maize domestication followed by a decrease to limited water availability in locally adapted varieties. By combining environmental and phenotypic association analyses with linkage mapping, we identified genes linking environmental variation and seminal root number. Functional characterization of the transcription factor *ZmHb77* and *in silico* root modelling provides evidence that reshaping root system architecture by reducing the number of seminal roots and promoting lateral root density is beneficial for the resilience of maize seedlings to drought .

## Main Text

The spread of crops and expansion of cultivation from their ancestral habitats were accompanied by substantial phenotypic changes driven by a combination of direct farmer selection and environmental adaptation (Meyer and Purugganan 2013). Maize (*Zea mays* ssp. *mays*) was initially domesticated in southwest Mexico approx. 9,000 years ago from the wild lowland teosinte *Zea mays* ssp. *parviglumis* with subsequent admixture with the highland teosinte *Zea mays* ssp. *Mexicana* contributing substantially to modern populations (Hake and Ross-Ibarra 2015; Yang et al. 2023). Following domestication from *parviglumis*, maize spread to the highlands of Mexico and South America (Ross-Ibarra and Piperno 2020; Fig. 1A). Subsequent adaptation to temperate climates allowed the expansion of maize from the tropics to diverse environments around the globe (Navarro et al. 2017; Swarts et al. 2017). Root system function is instrumental in colonizing new habitats (Ma et al. 2018) and acquiring resources, in particular water and nutrients in natural soils of different geographical origin (Eshel and Beeckman 2013). During domestication and diversification, the maize root system has become more complex by acquiring the capacity to form seminal roots, a feature largely absent in the maize progenitor teosinte (Hochholdinger et al. 2018; Lopez-Valdivia et al. 2022). In maize seedlings, the number of seminal roots determines the overall structure of the root system and thereby the depth and soil volume that roots can explore (Yu et al. 2016; Golan et al. 2018; Perkins and Lynch 2021). Seminal roots are formed endogenously in the embryo between 22–40 days after pollination (Hochholdinger et al. 2004). They are beneficial for nitrogen and phosphorus acquisition during maize seedling development (Perkins and Lynch 2021) and can persist and remain functional during the whole life cycle of the maize plant (Hochholdinger et al. 2004). Nevertheless, the question of how the maize root system adapted its form and function during domestication and global expansion remains elusive. However, understanding the genetic basis, environmental drivers and the potential adaptive value of seminal root number variation to changing environments is essential to develop crops resilient to future climatic challenges.

## Results

### Variation of SRN follows maize domestication

We investigated the environmental and genetic factors driving diversity in seminal root number (SRN) in the genus *Zea*. We quantified SRN in a set of >9,000 *Zea* accessions representing the worldwide diversity across the major maize cultivating regions in the Americas, Europe, Asia and Africa. Our collection included 173 wild teosinte accessions, 4,868 traditional varieties and 4,049 modern inbred lines. Under controlled conditions, maize varieties produced up to 11 seminal roots in traditional varieties (table S1) and up to 14 seminal roots in modern inbred lines (table S2). Overall, maize varieties formed on average 3.3 seminal roots, while teosinte accessions (Fig.1B and C) did not produce any seminal roots in 23% of the accessions ($n$ = 173) (fig. S1A; table S3). Interestingly, although SRN was low across all teosinte accessions, highland teosinte (*Zea mays* ssp. *mexicana*) produced significantly more seminal roots than the lowland teosinte *parviglumis* (fig. S1B). These data are consistent with the previously advanced hypothesis that seminal root formation in *Zea* is a domestication trait (Burton et al. 2013; Lopez-Valdivia et al. 2022).

Recently, it has been suggested that the increase of seed size during domestication was a prerequisite for seminal root formation (Perkins and Lynch 2021). In our study, SRN was only weakly correlated with seed size or the proportion of the embryo to the whole seed area across 2,429 modern inbred lines (fig. S2) and showed no relationship with embryo volume in a panel of diverse US traditional varieties (fig. S3). Thus, it is likely that the formation of seminal roots is independent from the process of seed selection during breeding. However, we cannot rule out the possibility that the other factors from the seed may have an effect on the SRN. To further investigate the relationship between seed traits and SRN, we evaluated an additional collection of 663 modern US inbred lines (table S4) and 975 globally distributed traditional varieties (table S5). We found that sweet corn, flour corn and popcorn varieties characterized by specific carbohydrate composition formed fewer seminal roots than other varieties in modern inbred lines (fig. S4A) or traditional varieties (fig. S4B). Analysis of near isogenic lines with mutants that alter the composition of the endosperm (*sugary1*, *shrunken2*) demonstrated that seminal root formation is independent of the amount of carbohydrates available during seed development (fig. S5). Thus, we hypothesize that the increase in SRN was part of domestication during the global expansion of maize, but was independent of seed traits in maize, which have been strongly modified by human selection and

breeding. It should be noted that sowing depth might have a potential effect on the variation of SRN, because modern varieties are usually planted closer to the soil surface than teosinte.

**Geographical and genomic signals of variation in seminal root number**

To determine whether and how SRN varies with environment, we applied machine learning to investigate the most important climatic and soil factors associated with SRN across 1,484 georeferenced traditional varieties sourced from diverse climatic and soil conditions (table S6). Traditional varieties which originated from arid regions had fewer seminal roots compared to those of other origins (fig. S6A). Using Random Forest modelling, we found that mean diurnal temperature range (MDR; Pearson's r = -0.36, $p < 0.001$), temperature seasonality (Pearson's r = -0.29, $p < 0.001$) and precipitation seasonality (Pearson's r = -0.07, $p = 0.010$) were the best environmental predictor of SRN followed by soil organic carbon (Pearson's r = 0.11, $p < 0.001$) and sand content (Pearson's r = -0.16, $p < 0.001$) (fig. S6B, C). High MDR and precipitation seasonality are important meteorological indicators associated with extreme climate such as deserts. Importantly, we further showed that paleoclimatic levels of precipitation in the mid-Holocene (ca. 6000 yrs ago) was a significant predictor of SRN (fig. S6D; Pearson's r = 0.30, $p < 0.001$), highlighting the importance of rainfall level in the evolutionary patterns of maize. To better understand the relationship between SRN and environment, we combined selected environmental variables into a second predictive random forest model. Focusing specifically on Mexican maize, we identified a broad trend of decreasing SRN with increasing latitude (Fig. 2A). We used our trained model to predict SRN for an additional panel of 1,781 previously genotyped and georeferenced Mexican varieties (Fig. 2A; Navarro et al. 2017). Using the available genotypes and our predicted SRN values, we performed a genome wide association study (GWAS; Fig. 2B), identifying genomic loci linked to the combinations of environmental variables that themselves described SRN variation in our training set.

To phenotypically map SRN in Mexican maize, we generated and evaluated an eight-parent Multi-parent Advanced Generation InterCross (MAGIC) population generated from founders that spanned the previously observed latitudinal cline in SRN (Fig. 2C). Comparison of the results of predicted trait GWAS and MAGIC mapping identified several shared genomic regions, including a locus on chromosome 1 linked to the previously described gene *rootless concerning crown and seminal roots* (*rtcs*; Fig. 2B; Taramino et al. 2007). The MAGIC population partially breaks down the population structure that can confound studies of local adaptation. On this basis, we used the MAGIC families to generate a genome wide predictive model for SRN and then applied this model to the eight founder haplotypes. Interestingly, our model recovered the latitudinal trend in SRN that we have observed in our broader sampling (Fig. 2D). This result was robust to the removal of any single chromosome from the model, indicating that effects throughout the genome were contributing to the clinal trend, consistent with persistent directional selection and local adaptation. We examined more closely the region of the genome around *rtcs* by modelling separate allele effects for each of the eight founders, recovering evidence of an allelic series with effects ranging from positive to negative following the founder source from South to North (Fig. 2E). Thus, our ecological and genomic models suggest SRN variation is likely shaped by indirect selection for adaptation to new environments.

**Northern Flint drive seminal root differentiation**

Previous population genetic analyses have described the expansion of maize out of Northwestern Mexico and its subsequent adaptation to the dry environment of the Southwestern US (Arizona and New Mexico) (Merrill et al. 2009; da Fonseca et al. 2015). In our study, accessions sampled from the Southwestern US had remarkably low SRN (Fig. 3A). In fact, more than 57% (53/92) of Southwestern US accessions completely lacked seminal roots (Fig. 3B; table S2). Such seminal root defective phenotypes from the Southwestern US were more drastic than those of the investigated teosinte lines (fig. S1A; table S1). Interestingly, we observed such low SRN exclusively in the United States, Canada and some European countries (table S1), which associates with a higher share of Northern Flint, a group derived from the US Southwest (Doebley et al. 1986; Rebourg et al. 2003; Hu et al. 2021). Using a maximum-likelihood estimation, we evaluated the effect of Northern Flint germplasm on SRN across our sampling. We found that the proportion of alleles derived from Northern Flint germplasm negatively correlated with SRN in both the US (Fig. 3C) and modern European inbred lines (Fig. 3D). SRN was not significantly correlated with proportions of germplasm derived from Tropical highlands, Tropical lowlands or Southern dent (fig. S7). We next genotyped 778 geographically diverse US traditional varieties and confirmed that the proportion of introgressed Northern Flint germplasm correlated negatively with SRN (Fig. 3E). We also evaluated a collection of introgression lines carrying genomic regions of the typical

Northern Flint traditional variety Gaspé Flint (Salvi et al. 2011). The introgression lines with higher share of the Northern Flint genome formed fewer seminal roots than the other panels evaluated (fig. S8). Overall, these phenotypic and genetic analyses indicate that alleles derived from Northern Flint germplasm of Southwestern US origin are an important factor determining SRN during the local adaptation of maize to different environments.

**Seminal root variation contributes to root functional traits**

To determine the potential adaptive importance of SRN across different environments, we used *in silico* root models to determine the impact of SRN in the context of whole root system architecture using 218 representative US maize traditional varieties (table S7). We first evaluated root architectural and morphological traits using a rhizobox system (Osthoff et al. 2019) to parameterize the structural-functional model CPlantBox (Zhou et al. 2020). The simulations illustrate that SRN negatively correlates with seedling primary root length and lateral root density along the primary root throughout the whole root system (Fig. 4A). We found that variation in SRN impacts seedling vigour by modulating the overall root system conductance, Krs (Fig. 4B). To explore whether changes in SRN will reshape root system architecture under realistic soil conditions, we used magnetic resonance imaging and positron emission tomography (MRI-PET) to compare the maize seminal rootless mutant *rtcs* to an isogenic wild type line that produced an average of three seminal roots (Fig. 4C). In the absence of seminal roots, the *rtcs* mutant produced an increased number of lateral roots. Water uptake in young maize has previously been shown to be dominated by lateral roots (Ahmed et al. 2016), suggesting that reducing in SRN to favour lateral root production may have an adaptive advantage for seed establishment in water limited conditions. We further characterized a specific Southwestern US traditional variety that we had identified to produce very few seminal roots but an enhanced number of lateral roots (Fig. 1C and S9). Thus, variation in SRN might drive the overall dimension and branching of whole root system, which will potentially determine the plant's capacity to capture water. We next used the CPlantBox realizations for each of the 218 traditional varieties to determine their standard uptake fraction (SUF) and demonstrated that the potentially relative contribution of lateral roots to total root water uptake decreases with increasing SRN (Fig. 4D). Based on these modelling results, variation in SRN might determine the overall absorptive surface by impacting lateral root formation.

We selected 66 representative traditional varieties (table S8) from the panel of 218 and experimentally measured transpiration rates in wet soil, finding no significant difference between groups (Fig. S10). We then used a soil-plant hydraulic model and determined that the stress onset limit (i.e., the point at which a small increase in transpiration provokes a large drop in leaf water potential at a given soil water potential), occurred at less negative leaf water potential in the traditional varieties with lower SRN (Fig. 4E). Actually, maize traditional varieties with one seminal root require higher water flow rates per unit root length than traditional varieties with five seminal roots, which induces a local drop in soil water potential and exhibits an earlier stomatal closure (Abdalla et al. 2022; Cai et al. 2022). This allows sustaining similar transpiration rates. We propose that such adaptive stomatal behaviour leading to lower transpiration is beneficial for seedling maize subjected to water stress. In addition, salt-simulated drought conditions tend to increase the lignin accumulation along the tip of the primary root (fig. S11). Interestingly, traditional varieties with less seminal roots tend to respond more dramatically than those with more seminal roots especially under water stress condition (fig. S11), which facilitates root penetration through dry soil (Schneider et al. 2021). Thus, seminal root variation might contribute to the optimization of root architectural, hydraulic and physiological changes for improved plant tolerance to limited water availability.

***ZmHb77* regulates root system architecture and drought resilience**

To understand the genetic basis of variation in SRN in inbred maize, we performed GWAS using an association panel of 1,604 diverse modern inbred lines, which are mainly originating from the US, China and Europe and cover the maize heterotic groups used in the US and China (Li et al. 2022). We observed substantial variation in SRN, with values ranging from 0 to 12 with an average of 3 (table S3). We detected a total of 160 associated SNPs ($p$ = 1.0e–05), corresponding to 160 candidate genes underlying SRN (Fig. 5A, table S9). Among these candidate genes, we identified *rtcs*, which is known to regulate SRN in maize (Taramino et al. 2007). We next screened for novel mutants of these candidate genes in the *BonnMu* reverse genetics resource of maize (Marcon et al. 2020), and identified transposon

insertions in 5 distinct genes that resulted in reduced SRN (fig. S12; table S10). Among those five genes, one gene Zm00001d045398 on chromosome 9 was annotated as *Homeobox-transcription factor 77* (*ZmHb77*; Qiu et al. 2022). To further validate the function of *ZmHb77* in regulating root development, we generated two independent CRISPR/Cas9 knockout lines (KO#1 and KO#3) (Fig. 5B). Both mutant alleles KO#1 and KO#3 conditioned a significant reduction in SRN (Fig. 5C-D) coupled with an increase in lateral root density (Fig. 5E-F), suggesting that this gene plays a role in reshaping seedling root architecture by regulating SRN and lateral root density. Specifically, the haplotype analysis suggested that Hap 1 contributes to significant more seminal roots than the other haplotypes (Fig. 5G). We then carried out a soil cultivation box experiment with mutant and wild type plants under well-watered and drought conditions followed by re-watering. The mutants showed a significant advantage regarding growth and photosynthesis rate under both drought and re-watering conditions, although there were no visible differences under well-watered conditions (Fig. 5H-K). Interestingly, mutants with fewer seminal roots but more lateral roots were more tolerant to drought and have a higher survival rate than wild type plants after re-watering, while we observed no differences between mutants and wild type under well-watered conditions (Fig. 5H, L). These results support the notion that *ZmHb77* controls SRN and that SRN-dependent root architectural traits, in particular lateral root density improve drought tolerance as well as the recovery of drought stress.

**Natural variation of the *ZmHb77* allele and function**

To explore the natural variation of *ZmHb77* in association with root architecture and drought tolerance, we first aligned our structural-functional model results to georeferenced locations across the US. Interestingly, root system hydraulic conductance showed a general gradient pattern from the Southwest dry area to the temperate region of the US (Fig. 6A), suggesting that root hydraulic conductance might have adapted with water availability. We then extended our drought analysis to the different traditional varieties and verified that Northern Flint varieties ($n$ = 5) with less seminal roots contribute to drought tolerance and resilience (fig. S13A) and showed a significantly higher biomass (fig. S13B) and stomatal conductance (fig. S13C) after re-watering. We next performed the haplotype analysis for *ZmHb77* allele in the traditional varieties and identified 41 high-confidence haplotypes (C allele) and the same number of A allele haplotypes (table S11). In particular, C allele haplotypes displayed significantly less seminal roots but significantly higher drought tolerance than the A allele haplotypes (Fig. 6B).

To further identify potential isogenic lines carrying the *ZmHb77* allele and drought tolerance based on Northern Flint sourced varieties, we evaluated the SRN, lateral root density and dry biomass under well-watered and drought conditions for the whole Gaspé Flint introgersson library introgressed into B73 (Salvi et al. 2011, 2021). We first demonstrated that GF111 (inbred line developed by repeated selfing and selected from Gaspé Flint) had a great advantage with respect to drought tolerance and resilience in comparison to the inbred B73 (Fig. 6C). Next, we explored the whole introgression population ($n$ = 71) and identified that the lines with a higher share of the GF111 genome showed significantly ($R^2$ = 0.12, $P$ = 0.0015) less seminal roots, but significantly ($R^2$ = 0.38, $P$ = 7.3e−09) higher lateral root density (Fig. 6D). At the same time these genotypes provided drought tolerance as measured by the drought index of the dry biomass. Specifically, we identified four introgression lines ($GF111^{ZmHb77}$) with *ZmHb77* alleles from GF111 and another four lines ($B73^{ZmHb77}$) from B73, respectively. The $GF111^{ZmHb77}$ lines formed less seminal roots but a significantly higher lateral root density than the $B73^{ZmHb77}$ lines (Fig. 6D). We then performed an RNA sequencing experiment to explore the gene expression pattern in the embryo and root stele tissue. Interestingly, *ZmHb77* is in general lowly expressed in the embryo tissue but highly expressed in the root stele, where the lateral roots initiated (Fig. 6E), suggesting that the major function of *ZmHb77* is linked with lateral root formation. Based on the specific expression pattern of *ZmHb77* between the $GF111^{ZmHb77}$ and $B73^{ZmHb77}$ lines, *ZmHb77* might function in the promotion of seminal root formation but inhibition of lateral root density in maize seedlings (Fig. 6E). In particular, $GF111^{ZmHb77}$ lines displayed a strong drought tolerance as highlighted by a higher photosynthetic rate and stomal conductance (Fig. 6F, fig. S14). Indeed, less inhibition of *ZmHb77* on lateral root formation was demonstrated in the $GF111^{ZmHb77}$ lines under drought followed by re-watering (Fig. 6G). Interestingly, drought tolerance in maize driven by root architectural changes can be independently validated by the *rtcs* mutant and its wild type (fig. S15). Finally, we summarized our finding as a schematic model in which *ZmHb77* acts as a central modulator contributing to the promotion of seminal root formation but inhibition of lateral root density in maize seedlings. Such root architectural and functional plasticity provides maize seedlings a great potential to balance the external water constraints.

## Discussion

Plant root system architecture plays a critical role in the adaptation to environmental constraints (Giehl and von Wirén 2014; Ma et al. 2018). To date, little is known on how the formation and function of root systems evolved in space and time during domestication of agricultural crops. Nonetheless, it has remained unclear to what extent root trait adaptation was required to introduce maize to new environments and what role root traits played in maize domestication. Using the global diversity of the genus *Zea*, our study demonstrates that SRN varies between domesticated maize traditional varieties and modern inbred lines compared with their wild teosinte progenitors and suggests that variation of SRN might have played an overriding role during the process of maize domestication (Fig. 1; Lopez-Valdivia et al. 2022). In traditional maize varieties, the demographically distinct groups sweet corn, flour corn and popcorn sourced from Southwestern US have shown the fewest SRN (fig. S4). Independent lines of evidence indicate that adapted alleles derived from Northern Flint maize contribute to the variation of SRN in both modern inbred lines and traditional varieties (Fig. 3). Subsequent local adaptation of SRN is in line with the maize domestication history, in which Northern Flint originated from the Southwest US desert (Merrill et al. 2009; da Fonseca et al. 2015), and then expanded to the northern US and Europe (Tenaillon and Charcosset 2011). We further applied ecological and genomic models and found a clinal trend in SRN across latitude and climatic factors (Fig. 2A; fig. S9). Recently, such an adaptive signature has been reported in the geographical adaptation of rice to local soil nitrogen availability (Liu et al. 2021). Here, we provide evidence for *rtcs,* a known determinant of SRN, to associate with variation in SRN along geographical gradients (Fig. 2E), emphasizing the importance of landscape and environmental factors in driving root trait differentiation.

In the near future, climate change will increase the incidence of drought, imposing a major threat to crop production (Jägermeyr et al. 2021). Improved adaptive capacity to flash drought is required for crops to mitigate such negative impacts in agricultural systems (Yuan et al. 2023). To tolerate stress and optimize the uptake of water even with a transient drought period, crops need to adapt root properties. We detected enhanced lateral root branching in both traditional varieties (Fig. 1C) and the *rtcs* mutants when seminal roots were absent (Fig. 4C), as well as recovering a similar result through *in silico* modelling (Fig. 4A). At the seedling stage, traditional varieties with fewer seminal roots can substantially reduce the carbon cost for the seed, and thus enable formation of highly dense and long lateral roots along the primary root (Fig. 4). Interestingly, we detected a significantly higher accumulation of lignin in the primary root tip of traditional varieties with few or no seminal roots under osmotic stress conditions (fig. S14). Such adaptive behaviour with enhanced lateral root branching in contact to water (Ahmed et al. 2016) and primary root lignification for better penetration of hard and dry soil (Schneider et al. 2021) improves plant tolerance to limited water availability, especially for the survival of seedlings after severe drought (Wang et al. 2016). In this context, we identified the transcription factor *ZmHb77* that affects overall root architecture by suppressing SRN but increasing lateral root density (Fig. 5C-F). Deletion of *ZmHb77* ultimately enhances survival of plants after recovery from drought (Fig. 5J, L). Indeed, domesticated wheat and barley have also been reported to form a larger number of seminal roots than their wild relatives (Grando and Ceccarelli, 1995; Golan et al. 2018). Based on the global warming scenario and an increasing incidence of drought, it is necessary to consider reducing the number of seminal roots in favour of lateral root branching for more efficient acquisition of soil water in the modern cultivars. It is important to note that such architectural plasticity will have its major impact during the seedling stage before crown roots become established (Hochholdinger et al. 2018) and sustain water uptake at later developmental stages. Our systemic analyses indicate that SRN is an important driver for the formation and pattern of lateral roots along the primary root (Fig. 6), thereby determining the overall absorptive surface and foraging capacity of crop roots. Variation in SRN alters hydraulic properties and may bear genetic potential to modify root plasticity and deepen our understanding of how plant roots sense and adapt to fluctuating water availability by hydropatterning (Orosa-Puente et al. 2018) or xerobranching (Mehra et al. 2022). Future studies need to address how SRN variation can optimize root development and hydraulic architecture for enhanced resilience in cereals (Maurel and Nacry 2015). Our results do not only reveal the past signature of domestication and adaptation of maize roots, but highlight the genetic potential to improve climate resilience in future crops.

## Main figures

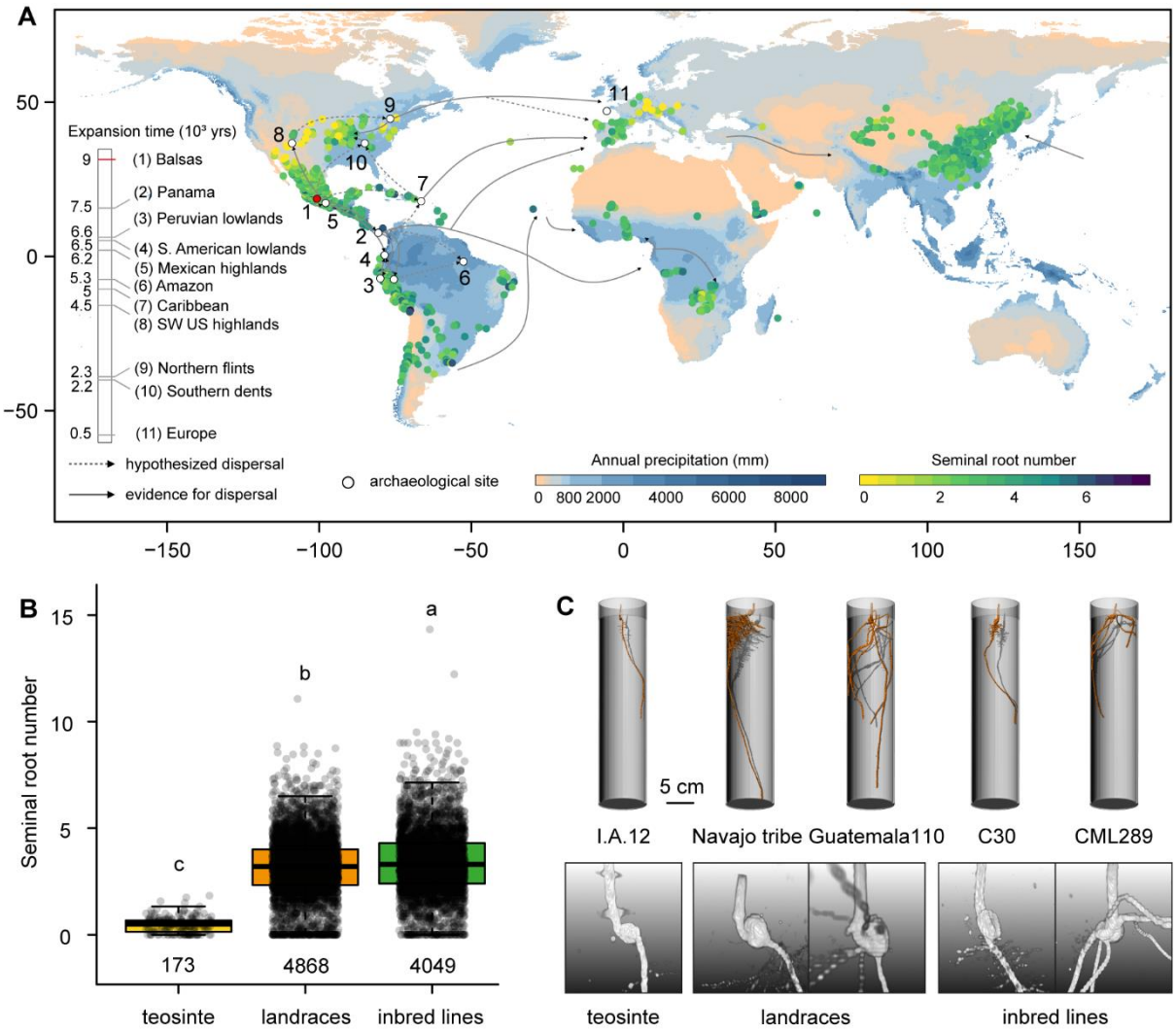


**Main figure 1. Maize evolutionary history resolves global organization of seminal root number (SRN). A**, Geographical variability of SRN in maize traditional varieties (*n* = 2424). SRN was determined in globally collected traditional varieties of indicated geographical origin. Domestication and expansion times for maize populations are indicated according to Ross-Ibarra and Piperno 2020. The global map of average annual precipitation between 1991 and 2020 is derived from NOAA Climate.gov. Dot colours from yellow to blue correspond to increasing SRNs. Solid arrows indicate the current evidence for global maize dispersal. Dashed arrows indicate hypothesized dispersal. White dots indicate locations of archaeological sites. **B**, Seminal root differentiation across the genus *Zea* including teosinte, traditional varieties and modern inbred lines. Each dot indicates the average SRN of each investigated accession. Number of analyzed seedlings per genotype: modern inbred lines *n* = 10; traditional varieties *n* = 20. Boxes span from the first to the third quartile, lines represent the median and whiskers include data within the 1.5× interquartile range of the lower and upper quartiles. Data points outside of whiskers represent outliers. Significant differences among groups are indicated by different letters (ANOVA, Tukey's HSD, $p = 0.001$). **C**, Reconstruction of root system architecture and initiation sites of seminal roots by non-invasive magnetic resonance imaging (MRI) in natural soil. Teosinte: I.A.12 (Ames 21793); Traditional varieties: Navajo tribe (PI 311229); Guatemala 110 (PI 490825); Modern inbred lines: C30 (Ames 26815); CML289 (Ames 32336).

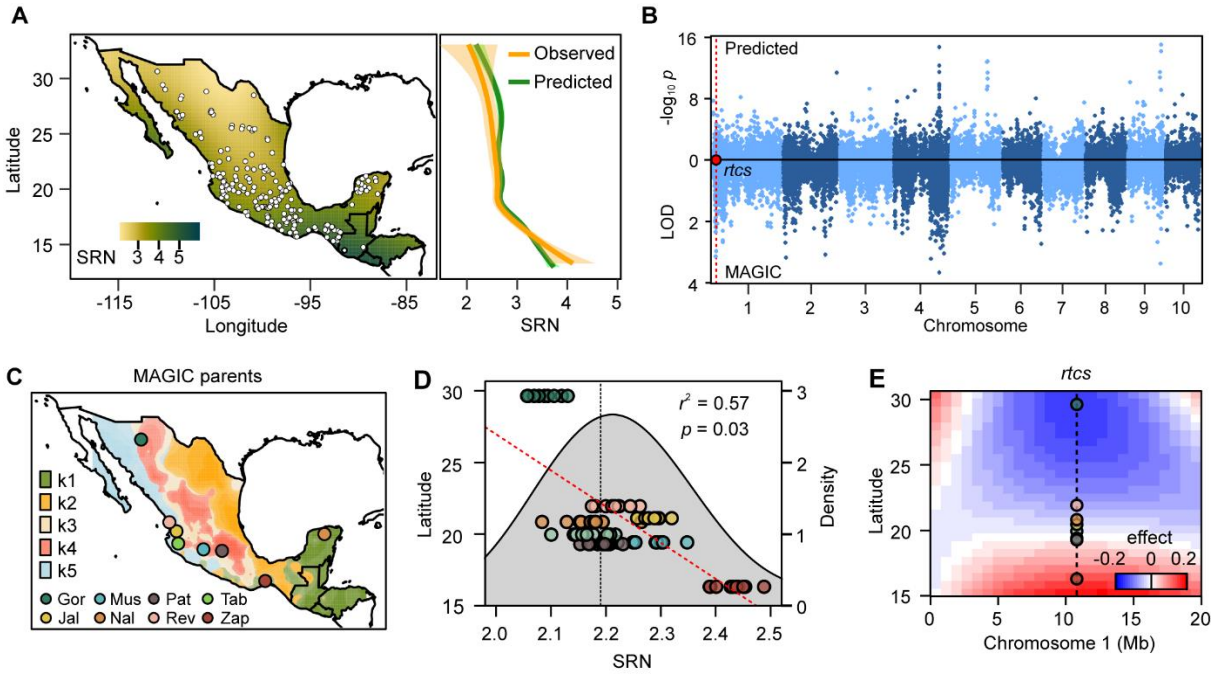


**Main figure 2. Geographical and genomic signatures of SRN variation in Mexico. A**, SRN decreases along a latitudinal gradient from South to North in Mexico. White dots indicate locations of sampled native maize traditional varieties. Green saturation indicates increasing predicted SRN based on a Random Forest model. The marginal plot depicts the calculated means of observed and predicted SRN over latitude. **B**, Genomic loci of SRN variation. Miami plot shows GWA of SNPs predicted trait values above the x-axis and with measured traits from a MAGIC population below the axis. Alternating colours indicate the ten maize chromosomes. The *rtcs* gene was labelled accordingly. **C**, Source of the eight founders of the MAGIC population. Shading on the map corresponds to an ancestry coefficient (K = 5) based on a broader genotyped panel. LOD, logarithm of odds. MAGIC founder traditional varieties abbreviations: Gor, Gordo; Mus, Mushito; Pat, Palomero Toluqueno; Tab, Tablonicllo; Jal, Jala; Nal, Nal Tel; Rev, Reventador; Zap, Zap Chico. **D**, Genome-wide effects in the MAGIC population support a latitudinal dependency of SRN. Dots show predicted SRN for each of the eight founder parents based on a genome wide model generated from the derived MAGIC families. Multiple points for each founder indicate the result of dropping each chromosome in turn from the model. The trend line and correlation are based on the complete model using all ten chromosomes. The grey curve shows the frequency density of the whole population with the vertical line at the mean. **E**, MAGIC founder allele effects in a 20 Mb window around *rtcs*. Polynomial fit of marker effects against source latitude for the eight alleles segregating in the MAGIC population. The vertical dashed line indicates the position of *rtcs*.

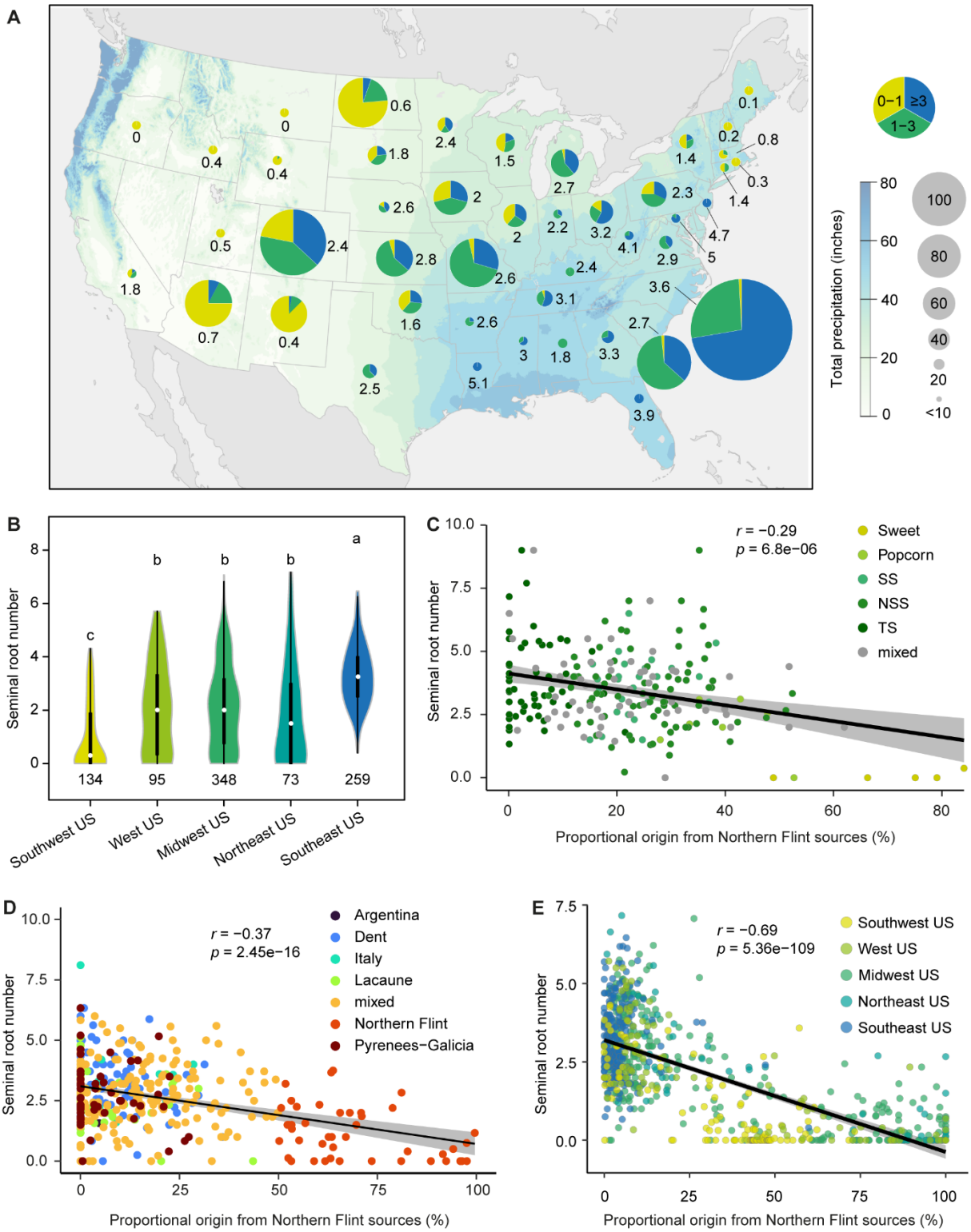


**Main figure 3. Variation in seminal root number coincides with proportional origin from Northern Flint maize sources. A**, Patterns of water availability and seminal root differentiation across the US. The annual average precipitation (1991-2020) map is derived from NOAA Climate.gov. The size of the pie charts indicates the number of sampled traditional varieties accessions while coloured areas denote proportions of SRN classes. **B,** Violin plots show SRN variation in traditional varieties originating from different geographical regions of the US. The traditional varieties accessions were contributed by NCRPIS and CIMMYT. The geographical information of groups of traditional varieties derives from the narrative information of the US National Plant Germplasm System (https://npgsweb.ars-grin.gov/gringlobal). Sample sizes are highlighted with exact numbers. Different letters indicate significant differences among regional pools (ANOVA, Tukey's HSD, $p$ = 0.001). Boxes span from the

first to the third quartiles, centre lines represent median values and whiskers extend 1.5× the interquartile range of the lower and upper quartiles. Significant differences among different groups are indicated by different letters (ANOVA, Tukey's HSD, $p = 0.001$). **C-D,** Correlation between SRN and the proportion of Northern Flint sources in the US Ames panel (**C**) and the European collection (**D**). Estimates of historical sources for individual Ames modern inbred lines and modern European inbred lines are extracted from Liu et al. (2003) and Gouesnard et al. (2017). Here, the proportion of Northern Flint sources was correlated with SRN across modern maize inbred lines. The *p* value denotes the probability at which the correlation coefficient is zero (null hypothesis). SS, stiff-stalk; NSS, non-stiff stalk; TS, tropical/sub-tropical; Mixed, mixture of these different germplasms. **E**, Correlation between SRN and the proportion of Northern Flint germplasm sources in US traditional varieties. The reference Northern Flint-sourced traditional varieties were defined according to Doebley et al. (1986). Scatter plots show combined SRN data of traditional varieties from different geographical origins with best fit (solid line) and 95% confidence interval (grey shading) for linear regression ($p = 5.4e{-}109$, $n = 778$). Different colours of dots correspond to different geographical origin of investigated traditional varieties.

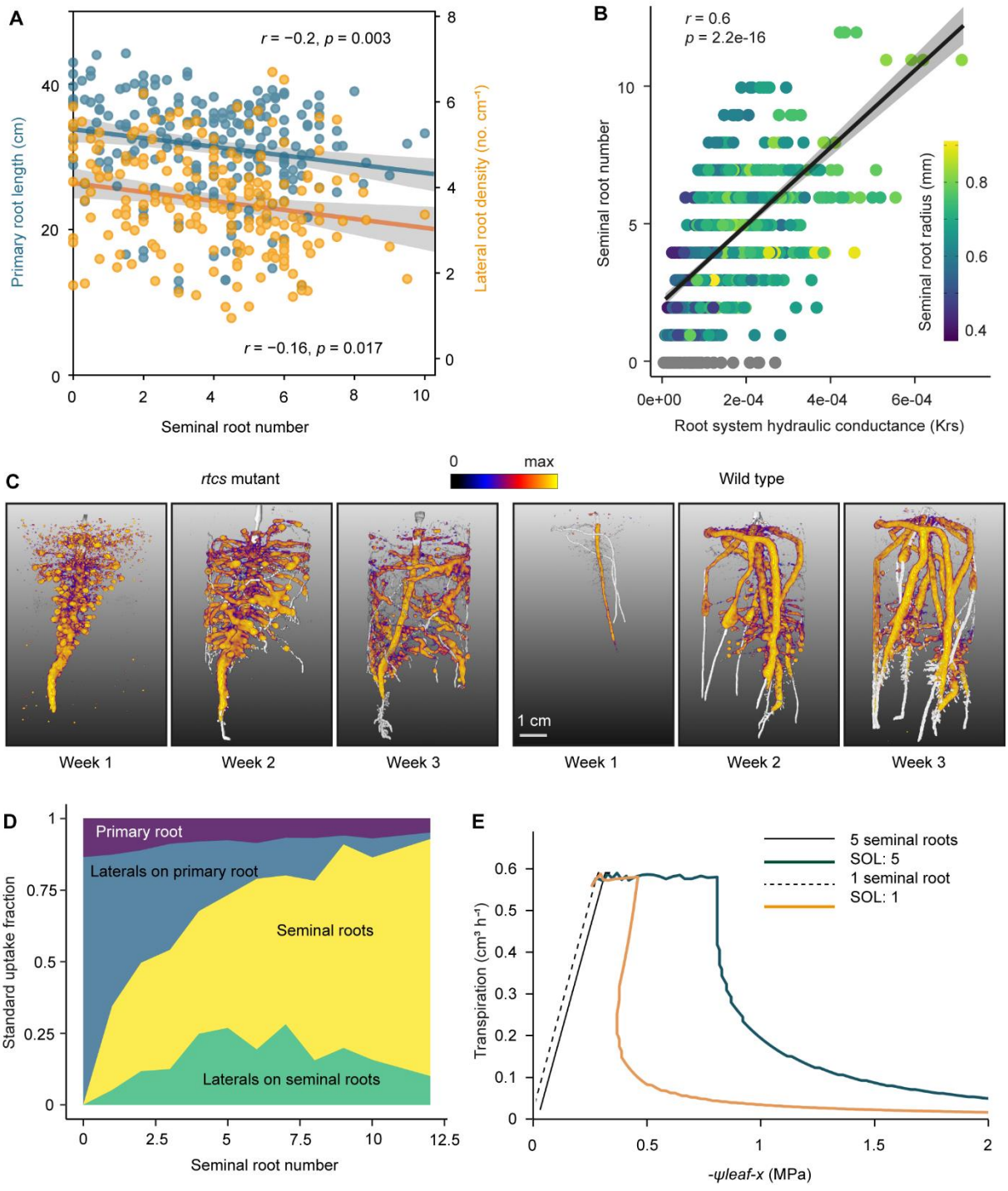


**Main figure 4. Variation in SRN drives overall root architectural and hydraulic properties. A**, SRN is negatively correlated with rooting depth of the primary root and lateral root density in different maize traditional varieties accessions grown in a rhizobox system. Scatter plots show combined seminal root data of traditional varieties grown in the rhizobox and linear regression with best fit (solid line) and 95% confidence interval (shaded area) (*n* = 218). **B**, Seminal root variation affects overall root hydraulic properties. Root system conductance (Krs) is based on 2D images of root systems grown in the rhizobox and simulated root architecture by structural-functional modelling. **C**, Seminal root defects of the *rtcs* mutant cause highly branched lateral roots emerging from the primary root. Reconstruction of root architecture and carbon allocation by MRI combined with PET. Intensity of carbon deposition by radiolabelled $^{11}C$ is visualized by colour code. Note that when $^{11}C$ was supplied to leaves for the first time, the first two seminal roots were already formed. As MRI images were taken after the PET images,

growing root tips are not at the same position. **D**, Standard uptake fraction of seminal roots and lateral roots as a function of SRN. For each SRN the average proportion of water uptake per root type is expressed as a ratio relative to overall water uptake. The relative contribution to water uptake is considered separately for the primary root, lateral roots initiated from the primary root, total seminal roots and lateral roots initiated from seminal roots. Note that some of the traditional varieties with lower SRN already formed very short crown roots, but their contribution to water uptake is not considered. **E**, Simulation of transpiration rates of representative traditional varieties ($n$ = 76) from a subset of 218 traditional varieties. A maize traditional variety with one seminal root requires larger gradients in soil water potential than a traditional variety with five seminal roots to sustain the same transpiration rate. Hence stress onset limit (SOL) occurs at a lower negative leaf water potential for plants with lower SRN.

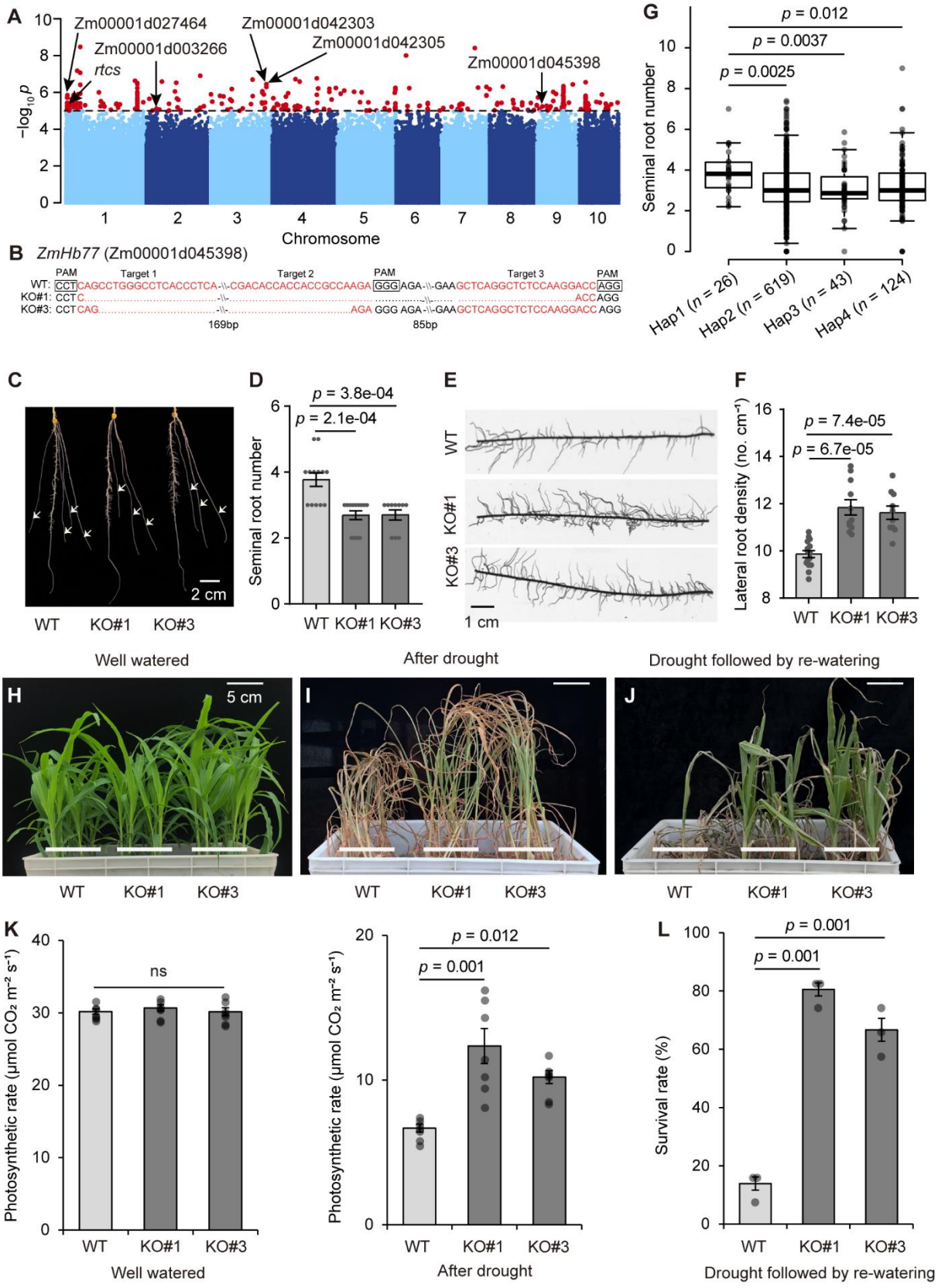


**Main figure 5. Functional characterization of *ZmHb77* controlling root traits and drought tolerance. A**, Manhattan plot from GWA mapping of SRN in 1,604 diverse modern inbred lines. The dashed horizontal line represents the suggestive threshold ($p$ = 1.0e–05). The known gene *RTCS* and five novel candidate genes controlling SRN are indicated by arrows. **B**, Sequence of *ZmHb77* and the target sites of mutation by CRISPAR/Cas9. PAM, protospacer-adjacent motif. CRISPR-knockout (KO#1 and KO#3) plants of *ZmHb77* display lower SRN (**C, D**) but higher lateral root density than the wild type

(WT) (**E, F**). Root phenotyping was performed for two-week-old maize plants grown in the paper rolls. SRN was counted and lateral root density was obtained from the number of lateral roots per cm of primary root. At least ten individual plants were examined for root traits. **G,** Haplotype analysis of maize inbred lines. Comparison of drought tolerance between WT and plants of the two *ZmHb77* CRISPR knockout lines grown under well-watered (**H**), drought (**I**) and drought followed by re-watering (**J**). **K**, Photosynthetic rate of mutants and wild type under well-watered and drought conditions. (**L**) Survival rate of WT and *ZmHb77* knockout lines after exposure to drought stress. Wild type and mutant seeds were precultured under well-watered conditions until three-leaf stage, and then either adequately supplied with water or not watered for another twelve days. Drought-stressed plants were re-watered and the survival rate was recorded after seven days. Three biological replicates were performed and each replicate included twelve individual plants. Significant differences between WT and KO lines are indicated by indicated *p* values (one-sided Student´s *t*-test). ns, not significant.

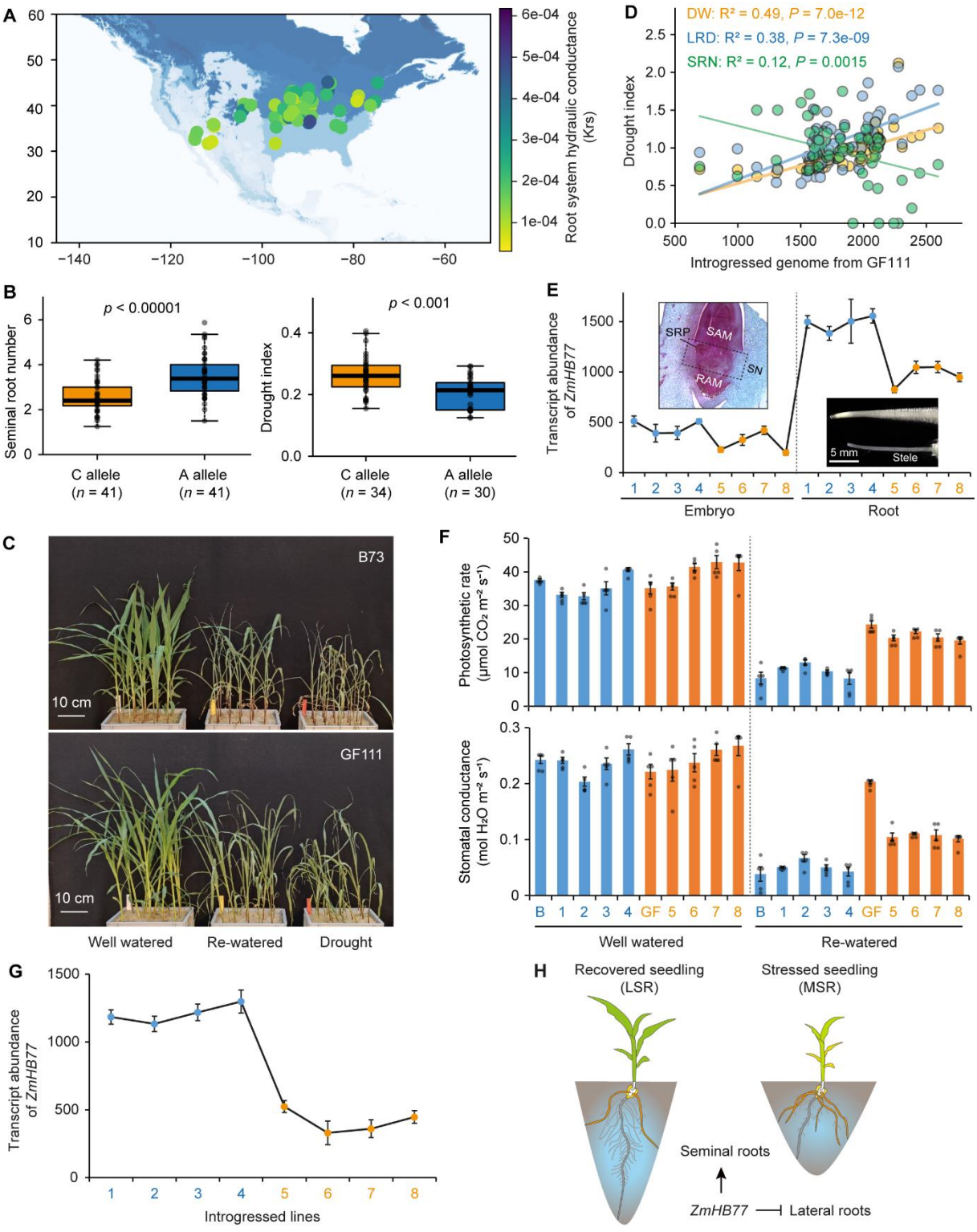


**Main figure 6. Natural variation of the *ZmHb77* allele and its contribution to root architecture and drought tolerance in maize seedlings. A**, Geographical distribution of root system hydraulic conductance. Each data point corresponds to the structural-functional model outcome. **B**, Haplotype analysis for traditional maize varieties. Boxes span from the first to the third quartile, lines represent the median and whiskers include data within the 1.5× interquartile range of the lower and upper quartiles. Data points outside of whiskers represent outliers. **C**, Seedling performance of B73 and GF111 (inbred line developed by repeated selfing and selected from Gaspé Flint) grown under well-watered, drought and drought followed by re-watering. **D**, Correlation between drought index and the proportion of introgressed genome from GF111. SRN, seminal root number; LRD, lateral root density; DW, dry weight. **E**, Tissue specific expression of *ZmHb77* in the embryo and root stele between different introgressed

lines from B73 (1−4) and GF111 (5−8) donors. SAM, shoot apical meristem; RAM, root apical meristem; SN, scutellar node; SRP, seminal root primordia. **F**, Photosynthetic rate and stomatal conductance of different introgression lines from B73 and GF111 donors under well-watered and re-watered conditions, respectively. **G**, Expression of *ZmHb77* in the root stele tissue after re-watering among different introgression lines. **H**, Working model of a potential function of *ZmHb77* on the formation of seminal roots and lateral roots in contribution to maize seedling drought tolerance. MSR, more seminal roots; LSR, less seminal roots.

## References and notes


K. Swarts *et al*., *Science* **357**, 512−515 (2017).

J. F. Doebley, M. M. Goodman, C. W. Stuber, *Am. J. Bot.* **73**, 64–69 (1986).

R. R. da Fonseca *et al*., *Nat. Plants* **1**, 14003 (2015).

R. S. Meyer, M. D. Purugganan, *Nat. Rev. Genet.* **14**, 840–852 (2013).

S. Hake, J. Ross-Ibarra, *eLife* **4**, p.e05861 (2015).

J. A. Romero Navarro *et al*., *Nat. Genet.* **49**, 476–480 (2017).

G. Taramino *et al*., *Plant J.* **50**, 649–659 (2007).

K. Liu, M. Goodman, S. Muse, J. S. Smith, E. D. Buckler, J. F. Doebley, *Genetics* **165**, 2117–2128 (2003).

Y. Hu *et al., Nat. Commun.* **12**, 1227 (2021).

F. Hochholdinger, P. Yu, C. Marcon, *Trends Plant Sci.* **23**, 79–88 (2018).

C. Rebourg, M. Chastanet, B. Gouesnard, C. Welcker, P. Dubreuil, A. Charcosset, *Theor. Appl. Genet.* **106**, 895–903 (2003).

W. L. Merrill *et al*., *Proc. Natl. Acad. Sci. U.S.A.* **106**, 21019–21026 (2009).

A. Eshel, T. Beeckman, Eds., *Plant roots: the hidden half*. (CRC press, 2013).

Z. Ma *et al*., *Nature* **555**, 94–97 (2018).

L. Burton, K. M. Brown, J. P. Lynch, *Crop Sci.* **53**, 1042–1055 (2013).

G. Golan, E. Hendel, G. E. Méndez Espitia, N. Schwartz, Z. Peleg, *Plant Cell Environ.* **41**, 755–766 (2018).

C. Perkins, J. P. Lynch, *Ann. Bot.* **128**, 453–468 (2021).

I. Lopez-Valdivia *et al*., *Proc. Natl. Acad. Sci. U.S.A.* **119**, p.e2110245119 (2022).

C. Tötzke *et al*., *Sci. Rep.* **11**, 1–10 (2021).

M. A. Ahmed, M. Zarebanadkouki, A. Kaestner, A. Carminati, *Plant Soil* **398**, 59–77 (2021).

G. Cai, M. A. Ahmed, M. Abdalla, A. Carminati, *Plant Cell Environ.* **45**, 650–663 (2022)

H. M. Schneider *et al*., *Proc. Natl. Acad. Sci. U.S.A.* **118**, p.e2012087118 (2021).

C. Li *et al*., *Nat. Plants* **8**, 750–763 (2022).

C. Marcon *et al*., *Plant Physiol.* **184**, 620–631 (2020).

A. Osthoff *et al., BMC Genom.* **20**, 325 (2019).

P. Yu, C. Gutjahr, C. Li, F. Hochholdinger, *Trends Plant Sci.* **21**, 951–961 (2016).

X. Qiu *et al*., *Physiol. Mol. Biol. Plants* **28**, 425–437 (2022).

X. Zhou *et al*., *in silico Plants*, **2**, diaa001 (2020).

S. Salvi *et al., BMC Plant Biol.* **11**, 4 (2011).

J. Jägermeyr *et al., Nat. Food* **2**, 873–885 (2021).

X. Yuan *et al., Science* **380**, 187–191 (2023).

Y. Liu, *Nature* **590**, 600–605 (2021).

S. Grando, S. Ceccarelli, *Euphytica* **86**, 73–80 (1995).

M. I. Tenaillon, A. Charcosset, *C. R. Biologies* **334**, 221–228 (2011).

B. Orosa-Puente *et al*., *Science* **362**, 1407–1410.

P. Mehra *et al., Science* **378**, 762–768.

B. Gouesnard *et al*., *Theor. Appl. Genet.* **130**, 2165–2189 (2017).

R. F. Giehl, N. von Wirén, *Plant Physiol.* **166**, 509–517 (2014).
C. Maurel, P. Nacry, *Nat. Plants* **6**, 744–749 (2020).
J. Ross-Ibarra, D. Piperno, figshare. http://doi.org/10.6084/m9.figshare.12781307.v1 (2020).
N. Yang *et al*. *Science* **382**, 1013 (2023).

**Acknowledgements**

We thank Jeffrey Ross-Ibarra (University of California–Davis, USA) for reading and comments on the final version of the manuscript. We are grateful to the North Central Regional Plant Introduction Station (NCRPIS, USDA-ARS and Iowa State University, Ames, Iowa, USA) and the International Maize and Wheat Improvement Center (CIMMYT) for providing seeds for this work. NCRPIS is part of the USDA-ARS National Plant Germplasm System. We thank Alain Charcosset (GQE-Le Moulon, INRAE, Univ. Paris-Sud, CNRS, AgroParisTech, Université Paris-Saclay, Gif-sur-Yvette, France) and Manuel López Luaces (Centro Investigacións Agrarias Mabegondo, Spain) for contributing European maize germplasm. We thank Simon Mayer and Steffen Wagner (Leibniz Institute of Plant Genetics and Crop Plant Research, Gatersleben, Germany) for technical support for NMR and Stefan Ortleb, Laura Kalms, Philipp Hinrichs (Leibniz Institute of Plant Genetics and Crop Plant Research, Gatersleben, Germany) for image segmentation. R.K., D.v.D, R.M. and D.P. acknowledge support from the Helmholtz Association for the Forschungszentrum Jülich GmbH and thank Antonia Chlubek and Jonas Bühler for technical support by MRI and PET. We thank Antonia Chlubek, Gregor Huber and Jonas Bühler (Forschungszentrum Juelich GmbH, IBG-2) for technical support by MRI and PET. We thank Selina Siemens, Alexa Brox and Helmut Rehkopf (Crop Functional Genomics, INRES, University of Bonn, Germany) for root phenotyping and DNA extraction. This work is supported by the Deutsche Forschungsgemeinschaft (DFG) grants HO2249/22-1 to F.H. and YU272/1-1 to P.Y., 444755415 (Emmy Noether Programme) to P.Y., 403671039 (SPP2089 “Rhizosphere spatiotemporal organisation - a key to rhizosphere functions”) to F.H. and P.Y., 403641034 (SPP2089 “Rhizosphere spatiotemporal organisation—a key to rhizosphere functions”) to A.S., and Bundesministerium für Bildung und Forschung (BMBF) grant 031B195C to F.H. This work was partially funded by the Deutsche Forschungsgemeinschaft (DFG, German Research Foundation) under Germany's Excellence Strategy-EXC 2070 – 390732324. R.J.H.S. is supported by the USDA National Institute of Food and Agriculture and Hatch Appropriations under Project number PEN04734 and Accession number 1021929, Consejo Nacional de Ciencia Tecnologia (FOINS-2016-01) and National Science Foundation (No. 1546719). T.W. is supported by the National Key Research and Development Program of China (No. 2021YFD1200700, No. 2016 YFD0100103, No. 2020YFE0202300) and Innovation Program of Chinese Academy of Agricultural Sciences). The germplasm propagation is funded by the TRA Sustainable Futures (University of Bonn) as part of the Excellence Strategy of the federal and state governments. X.C. is supported by the Innovation Research 2035 Pilot Plan of Southwest University (No. SWU-XDZD22001). This work was also supported in part by the U.S. Department of Agriculture, Agricultural Research Service (USDA-ARS) to V.B.

**Author contributions:**

Conceptualization: F.H. and P.Y.
Supervision: F.H. and P.Y.
Methodology: F.H., P.Y., T.W. and R.J.H.S.
Investigation: P.Y., C.L., M.L., X.H., D.W., H.L., C.M., H.T., S.P., M.D., R.K., R.M., D. van D., D.P., L.B., I.P., M.F.R.R.J., S.S., A.A., M.A., M.A.A., F.M.B., A.S., G.L., A.H., K.S., L.S., C.M.M.
Funding acquisition: P.Y., F.H., X.C., T.W., R.J.H.S and A.S.
Writing – original draft: P.Y. and F.H.
Writing – review & editing: All authors.

**Competing interests:**

The authors declare no competing interests.